✚IJESRT

INTERNATIONAL JOURNAL OF ENGINEERING SCIENCES & RESEARCH TECHNOLOGY

INFLUENCES OF EXPANDED GRAPHITE ON THERMAL CHARACTERIZATIONS OF ERYTHRITOL, PARAFFIN, AND STEARIC ACID FOR LOW-TEMPERATURE PHASE CHANGE MATERIAL COMPOSITES

Bo-Kyung Choi[1,3], Jae-Kyoung Ko[2], Soo-Jin Park[3,*], Min-Kang Seo[1,*]
[1]R&D Division, Korea Institute of Carbon Convergence Technology, Jeonju 54853, Korea
[2]R&D Division, Korea Institute of Convergence Textile, Iksan 54590, Korea
[3]Department of Chemistry, Inha University, Incheon 55101, Korea

ABSTRACT

Phase change material (PCM) composites for latent thermal energy storage were made by mixing three different kinds of PCM (erythritol (Er), stearic acid (SA), and paraffin (Pa)) loaded with expanded graphite (EG) in liquid PCM with a mass fraction of 5, 10, and 20 wt%. The effect of EG on thermal behaviors of the PCM composites was evaluated. As a result, the thermal conductivity of the PCM composites increased with increasing the EG content. Among the three types of the PCM composites, EG/Er composites were observed to have relative enhancement up to 84.02% at 20 wt% EG content. However, the latent heat was somewhat decreased from 251.08 to 214.58 J/g owing to the presence of EG which caused the decrement of super cooling effect. Thermal cycling and thermal gravimetric analyses showed that the PCM composites had good thermal reliability and proper thermal stability. Therefore, the prepared PCM composites were appropriate for thermal energy storage applications because of their acceptable thermal conductivity, good thermal reliability, fast response speed, and proper thermal stability.

KEYWORDS: phase change materials, thermal energy storage, expanded graphite, thermal conductivity

INTRODUCTION

New and renewable energy sources are being investigated all over the world. The development of energy storage devices is as important as developing new energy sources. Thermal energy storage is considered as one of the most important advanced technologies, and a lot of attention has been paid to utilize the essential techniques for thermal applications ranging from heating to cooling [1-3]. Therefore, the latent thermal energy storage has become one of the most attractive techniques among the different methods used in thermal energy storage.

Phase change materials (PCM) have lately become a subject of active research for storing thermal energy and adjusting temperature by storing and releasing large amounts of latent heat during phase change process [4–6]. The applications of PCM in thermal energy storage have been well known in many fields, such as in solar energy storage, waste heat recovery, smart air conditioning in buildings, homothermal clothing, and so on. Therefore, considerable research efforts have been dedicated to improve the existing PCM and identify the new materials with desirable thermal properties [7-9].

PCM can be classified into two major categories: inorganic compounds and organic compounds. Inorganic PCM include salt hydrates, salts, metals and alloys, whereas organic PCM are comprised of paraffin, fatty acids, alcohols and glycols. Among the various kinds of PCM, erythritol, stearic acid, paraffin are taken as the most promising PCM because they possess desirable properties, such as high latent heat, non-toxicity, good chemical stability, easy availability [10-12]. However, they suffer from a low thermal conductivity, poor thermal stability, and liquid leakage when they undergo the solid–liquid phase change. These drawbacks reduce the rate of heat storage and extraction during the melting and solidification cycles and restrict their wide applications.

To overcome the problem relating to the low thermal conductivity of PCM, a great deal of efforts have been attempted, which include dispersing metallic or nonmetallic particles with high thermal conductivity into PCM [13-

15], using finned tubes with different configurations in a storage unit, and impregnating PCM into high thermal conductivity materials with porous structure, such as carbon materials and metal foams [16-18]. Compared with carbon materials, metal foams, additives or fins not only significantly increase the weight and cost of the storage systems, but also are incompatible with PCM for some of them.

The most popular method to enhance the thermal conductivity of PCM are adding high conductivity fillers, such as powders, metal foams, fibers, nanoplatelets, etc. Among them, carbon based materials, such as carbon nanofibers, carbon nanotubes, graphites are highly attractive as supporting materials owing to their low density, good thermal conductivity, chemical stability and wide availability. On the other hand, to minimize the loss of energy storage capacity resulting from the supporting materials, porous materials are considered as promising supporting materials. It is expected that the large surface area and low density of porous materials will enhance the shape stabilization capability and thus minimize the loss of energy storage capacity [19-21].

Recently, expanded graphite (EG) has been employed to enhance the heat transfer in PCM, due to its desirable properties of high thermal conductivity, high stability, low price, good compatibility with organic PCM, and lower density and weight as compared with metal promoters [22–25]. It has been shown that EG can improve the thermal conductivity of the PCM without much reduction in energy storage capacity and liquid exudation during its phase change. Lee et al [26] prepared EG/erythritol composites with various interlayer distance composites and then studied the effect of the additives of various interlayer distances of EG on thermal behaviors. As results, the thermal conductivity and the latent heat value significantly increased with an increase of EG interlayer distances. In particular, EG/ erythritol composites having the largest EG interlayer distance showed thermal conductivity of 3.56 W/mK and a latent heat value of 90 mass% of pure erythritol. In addition, Zhang and Fang [27] studied the effect of the EG addition on the thermal properties of the EG/Paraffin composites prepared as form-stable PCM, and they reported that the latent heat capacity of the PCM decreased with increase of the mass fraction of the graphite.

In this work, three different kinds of PCM (erythritol, stearic acid, and paraffin) composites containing the EG were prepared by impregnation method. The effects of EG on surface and structure properties, thermal conductivity, latent heat, thermal cycling, and thermal stability of the PCM composites were characterized by scanning electron microscope (SEM), transmission electron microscope (TEM), X-ray diffraction (XRD), thermal conductivity (TC), differential scanning calorimetry (DSC), and thermal gravimetric analysis (TGA).

MATERIALS AND METHODS
Materials
Erythritol (Cargill Co. with melting temperature of 118-130°C), stearic acid (Junsei Co. 64-71°C), and paraffin wax (Sigma-Aldrich Co. 53-57°C) were used as PCM and natural graphite (average diameter: 500 μm) was purchased from Sigma-Aldrich Co.

Preparation of EG
EG were prepared by a version of a previously reported method [28] ; graphite (10 g) was added into a mixture of sulfuric acid and nitric acid (4:1 volume rations). After 1 day reaction, the graphite obtained by filtration was washed with distilled water until a neutral pH was achieved, and then dried in a vacuum oven at 90°C for 8 h. The acid-treated graphite was treated at 900°C for 90 sec in a furnace. Table 1 provided the specifications of the erythritol, stearic acid, paraffin, and EG.

EG were composed of layered, but compactly fastened, and nanoplates of graphite, as shown in Fig. 1. It showed the worm- or accordion-like expanded structure of graphite intercalated compounds which were exfoliated up to about 500 times in its initial volume by rapid heating.
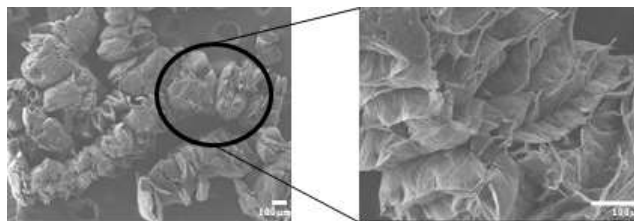

Fig. 1 SEM micrographs of EG

Table 1. Properties of erythritol, stearic acid (SA), paraffin, and expanded graphite (EG)

	Erythritol	SA	Paraffin	EG
Density (g/cm^3)	1.28	0.85	0.9	1.3
Thermal conductivity (W/mk)	0.34-0.73	0.33	0.356	4-200
Latent heat (J/g)	320-354	203	142.72	327
Melting point (^{o}C)	118-130	64-71	53-57	-

Preparation of PCM composites

The PCM composites were prepared by adding EG at different mass fractions into erythritol, stearic acid, and paraffin using the melting method [29]. The PCM was melted at over the melting temperature of each PCM, and the EG was then mixed into the liquid PCM. The PCM composites were prepared by stirring for 20 min at 100-200 rpm and sonication for 30 min of EG in liquid PCM with a mass fraction of 5, 10 and 20 wt%. Thermal conductivity would increase continuously with higher additive quantity of EG, but more than 20wt% EG were not added, because they have a very low weight density and low dispersibility. The PCM composites were cooled to the room temperature. Then, the PCM composites were obtained and labeled pure erythritol, EG/Er 5, EG/Er 10, EG/Er 20, pure stearic acid, EG/SA 5, EG/SA 10, EG/SA 20, pure paraffin, EG/Pa 5, EG/Pa 10, and EG/Pa 20. Fig. 2 showed the schematic diagram of manufacturing procedure of PCM composites.
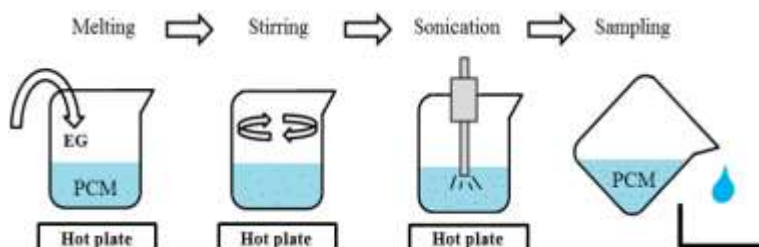
Fig. 2 EG Schematic diagram of manufacturing procedure for PCM composites.

Characterization

Scanning electron microscopy (SEM, S-4800, Hitachi) and transmission electron microscope (TEM, JEM 2100F, JEOL) were used to observe the surface morphology and microstructure of the PCM composites. For the TEM observations, the samples were dispersed in ethanol with a low power sonication-bath for a few minutes and deposited on a holey carbon coated copper by drying a droplet of a suspension on the grid. The XRD curves of the PCM composites were obtained using a PANalytical Model X'pert Powder diffractometer equipped with a rotation anode with CuKα radiation (λ=0.1542 nm) used to measure the interlayer spacing.

The latent heat of the PCM composites was obtained by differential scanning calorimeter (DSC, TA-60, SHIMADZU Co.). For DSC measurements, the amount of about 5.5 mg for every sample was sealed in an aluminum pan for characterization, at a heating rate of 10°C/min in a nitrogen atmosphere. The latent heat was calculated as total by numerical integration of the area under the peaks that represented the solid-solid and solid-liquid phase transition. The thermal conductivity was measured by Thermo Con Tester M100, Metrotech Co. Ltd., Korea. The thermal diffusivity of the PCM composites was measured by thermal diffusivity measurement apparatus (LFA447, NETZSCH). The samples with 12.7 mm diameter and 2 mm thickness were placed in the sample holders. The front side of a plane-parallel sample was heated by a short light pulse. The weight loss and thermal stability of

the PCM composites were obtained by thermogravimetric analysis (TGA, TGA-50, SHIMADZU Co.) at a heating rate of 20℃/min in temperature range of 30–600℃.

RESULTS AND DISCUSSION
Morphology of PCM composites
Fig. 3 showed SEM micrographs of the PCM composites. The EG remained in the worm-like structure after the erythritol was absorbed into the pores of the EG and the absorbed erythritol exhibited a uniform distribution in the PCM composites owing to the capillary force and the surface tension force of the porous EG. The EG with different mass ratios in the EG/SA composites was embedded and dispersed in the porous network of the EG. The two phases interfaces between the stearic acid and the EG combined compactly because of the high wetting ability of the stearic acid. The stearic acid exhibited a uniform distribution in the composites due to the effect of capillary and surface tension forces between the stearic acid and the porous network of the EG. The morphology and dispersibility of EG/Pa composites appear to follow the same trend.
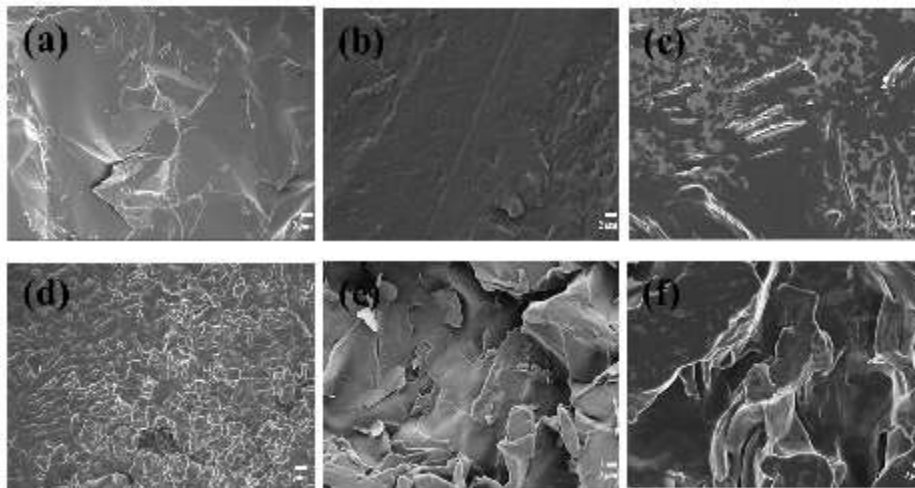

Fig. 3 SEM micrographs of (a) pure erythritol, (b) pure stearic acid, (c) pure paraffin, (d) EG/Er composites, (e)

EG/SA composites, and (f) EG/Pa composites

The more detailed structure of nanosheet was shown in Fig. 4. The nanosheets were dispersed in PCM matrix. After the PCM composites turned into solid, the well-dispersed EG nanosheets were fixed.
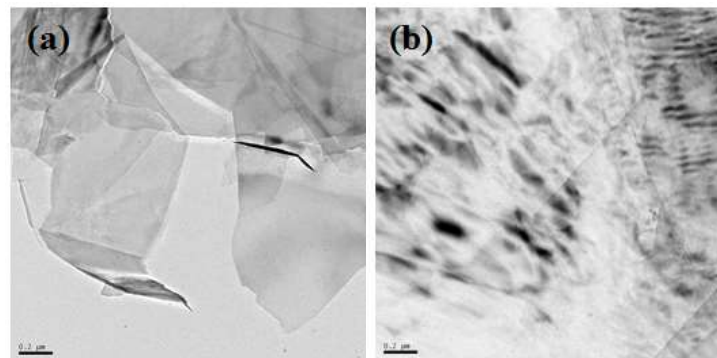

Fig. 4 EG nanosheet particles lying inside the erythritol matrix; (a) pure erythritol and (b) EG/Er 20

Structure of PCM composites

Fig. 5 showed the XRD curves of the PCM composites. A strong diffraction peak located at 26.5º (2θ) was observed in the XRD curve of the EG, attributed to the feature peak (002) of graphite. In the XRD curve of EG/Er composites, the same diffraction peak shifted to 26.66º and both declined and appeared wider because of the disorientation of the graphite sheets, as shown in Fig. 5(a). The XRD curve of EG/Er composites included the main diffraction peaks of pure erythritol, though the intensities of the peaks were lower than those of the corresponding peaks in the XRD curve of pure erythritol.

In the EG/SA composites, the XRD peaks at 21.5º and 23.9º were caused by the stearic acid, and the XRD peak of the EG in the PCM composites also appeared at 26.5º, in Fig. 5(b). The peak intensities of the peaks of EG/SA composites were lower than those of the corresponding peaks of pure stearic acid. This result indicated that the crystallite size of the EG became smaller in the composites due to the restriction of crystal of the stearic acid [30,31].

Similarly, in the XRD curve of EG/Pa composites (in Fig. 5(c)), the diffraction peak of (002) of graphite shifted to 26.44º and its intensity declined and appeared wider because of the disorientation of the graphite sheets. The XRD curves of the PCM composites contained all the peaks of paraffin and EG, whereas the peak intensities were relatively lower in comparison with those of paraffin and EG. These results suggested that the PCM composites were just the combination of paraffin with EG, and no new substance had been produced. It was due to the fact that the paraffin was hold by the capillary force and tension force of the porous EG, no liquid paraffin was observed on the surface of the PCM composites at the solid–liquid phase change process.
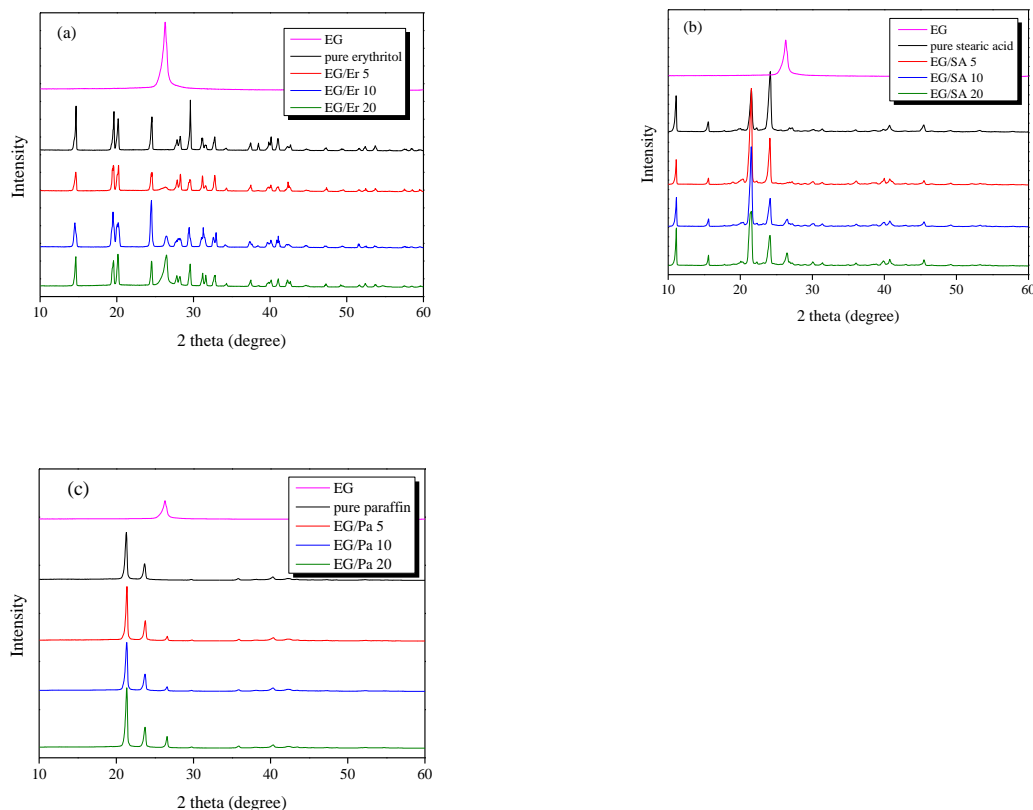

Fig. 5 EG nanosheet particles lying inside the erythritol matrix; (a) pure erythritol and (b) EG/Er 20 XRD curves of PCM composites as a function of EG content

Latent heat and thermal properties of PCM composites

DSC analysis was conducted to investigate the influence of EG addition on thermal properties, such as melting temperature (T_m) and the latent heat capacity of the PCM composites. The heating curves of the PCM composites from DSC measurements were presented in Fig. 6. Table 2 listed the melting points and the latent heat capacity of the PCM composites. The latent heat and T_m of pure erythritol were 251.08 kJ/kg and 125.2°C, respectively while the latent heat of EG/Er composites decreased to 230.99, 224.64, 190.65 kJ/kg and the T_m decreased to 126.5, 123.2, 116.2°C with addition of EG. Also, we could see from the heating curve in Fig. 6(c) that the paraffin had two phase change peaks. The first phase change peak at about 39.3°C was lower and corresponded to the solid–solid phase transition of the paraffin, and the second peak was very high at around 58.9°C, corresponding to the solid–liquid phase change. The latent heat of PCM and the PCM composites showed a decrease of latent heat with increasing the EG content which explained that the three-dimensional net structure confined heat movement [36,37].

Table 2. DSC data of pure PCM and PCM composites

| Samples	EG contents (wt%)	Melting temperatures (°C)	Specific heat (J/g·°C)	Thermal conductivity (W/mK)	Latent heat (J/g)
pure erythritol	-	125.2	2.01	0.745	251.08
EG/Er 5	5	126.5	1.96	0.831	245.34
EG/Er 10	10	123.2	1.92	1.174	240.67
EG/Er 20	20	116.2	1.72	1.371	214.58
pure stearic acid	-	72.00	1.44	0.342	180.54
EG/SA 5	5	71.43	1.36	0.409	170.46
EG/SA 10	10	71.33	1.39	0.518	173.28
EG/SA 20	20	70.63	1.27	1.577	157.83
pure paraffin	-	58.41	2.36	0.177	130.27
EG/Pa 5	5	58.74	2.24	0.188	122.73
EG/Pa 10	10	59.14	2.12	0.254	117.15
EG/Pa 20	20	58.11	2.09	0.313	116.09
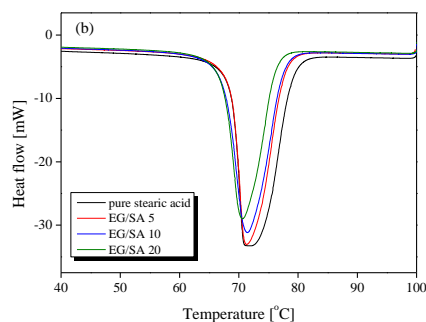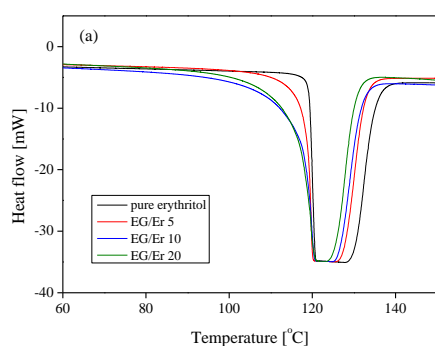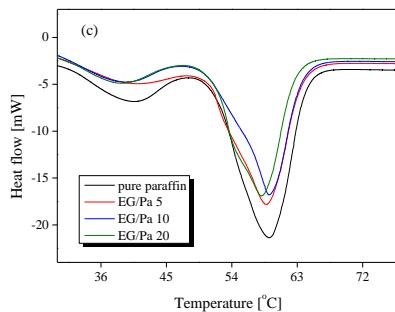
Fig.6 DSC curves of PCM composites as a function of EG content.

Thermal conductivity was measured by thermal equilibrium method according to the ASTM D 5470. It could be obtained from the temperature difference in response to an applied heating power, when the sample reached heat equilibrium with the copper rods in parallel to the sample to be measured by comparison with a reference material. The thermal conductivity was estimated by Fourier's law [32]:

$$Q = \frac{\lambda A}{d_A} \Delta T \qquad (1)$$

where, Q is the heat capacity, λ the thermal conductivity, A the direction normal to a unit surface area of copper rod, d_A the distance between upper and lower copper rods, and ΔT the temperature difference between sample surface and copper rods.

The change in thermal conductivity of the PCM composites with respect to the mass fraction of the EG was shown in Fig. 7 and Table 2. It could be seen that the thermal conductivity of the PCM composites clearly improved compared to that of pure PCM. Thermal conductivities of all PCM composites were linearly increased with increasing the EG content. Thermal conductivity of all pure PCM showed a significant increase by about 80–400% due to the addition of 20 wt% EG. However, although thermal conductivity of the PCM composites was increased, the latent heat of the PCM composites was somewhat decreased with EG content. It was reported that fillers could decrease the latent heat of the PCM composites because the dispersed fillers could interrupt the local boning environment of molecules and hinder the crystallization and melting of the PCM [33-35].
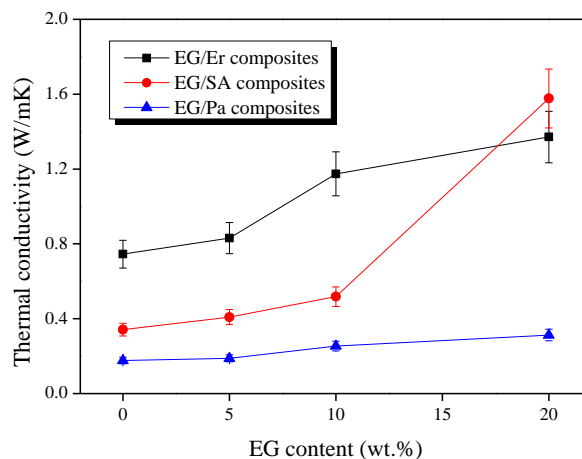

Fig.7 Thermal conductivity of PCM composites as a function of EG content

Thermal diffusivity was used to evaluate the response speed of the PCM composites in the environmental temperature change which was related to the heat transfer efficiency. The thermal diffusivity of the PCM composites were improved with increasing the EG content indicating the enhanced heat transfer efficiency [38,39], as shown in Fig. 8. Therefore, the PCM composites were recommended as promising composite materials because the thermal diffusivity of EG/Er 20, EG/SA 20, and EG/Pa 20 was 113.8%, 360.7%, and 76.3% higher than that of pure PCM, respectively.

We could conclude that the main advantage of the PCM composites with EG was the significant increase in thermal conductivity without much reduction in their latent heat energy storage capacity and without leakage of pure PCM even when it was heated over the melting temperature of pure PCM.
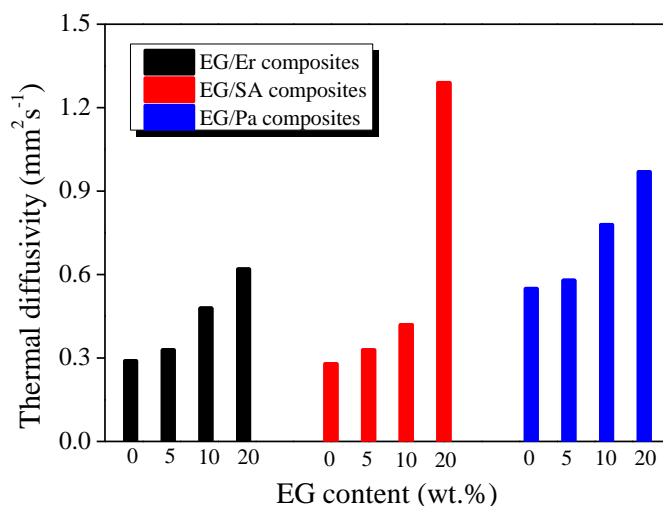

Fig.8 Thermal diffusivity of PCM composites as a function of EG content.

Thermal cycling of PCM composites

Fig. 9 showed latent heat changes of the PCM composites in the heating and cooling cycling tests. The latent heat values decreased drastically up to the 3rd cycle which was likely due to the leakage of the molten Er, SA, and Pa that was not embedded within the worm-like EG or in contact with it. In the subsequent cycles, the values remained almost constant indicating that was very little further leakage from the composites. Thermal cycling results showed that the shape stabilization of Er, SA, and Pa was achieved by adding only 20 wt% of EG and there was no leakage of PCM after exposure to 5 cycles.

Based on the results we could conclude that the form stable PCM composites had good thermal reliability with regarding to the changes in its phase change temperatures and latent heats. Their excellent cycling performance was of great importance in their prospective thermal energy storage applications.
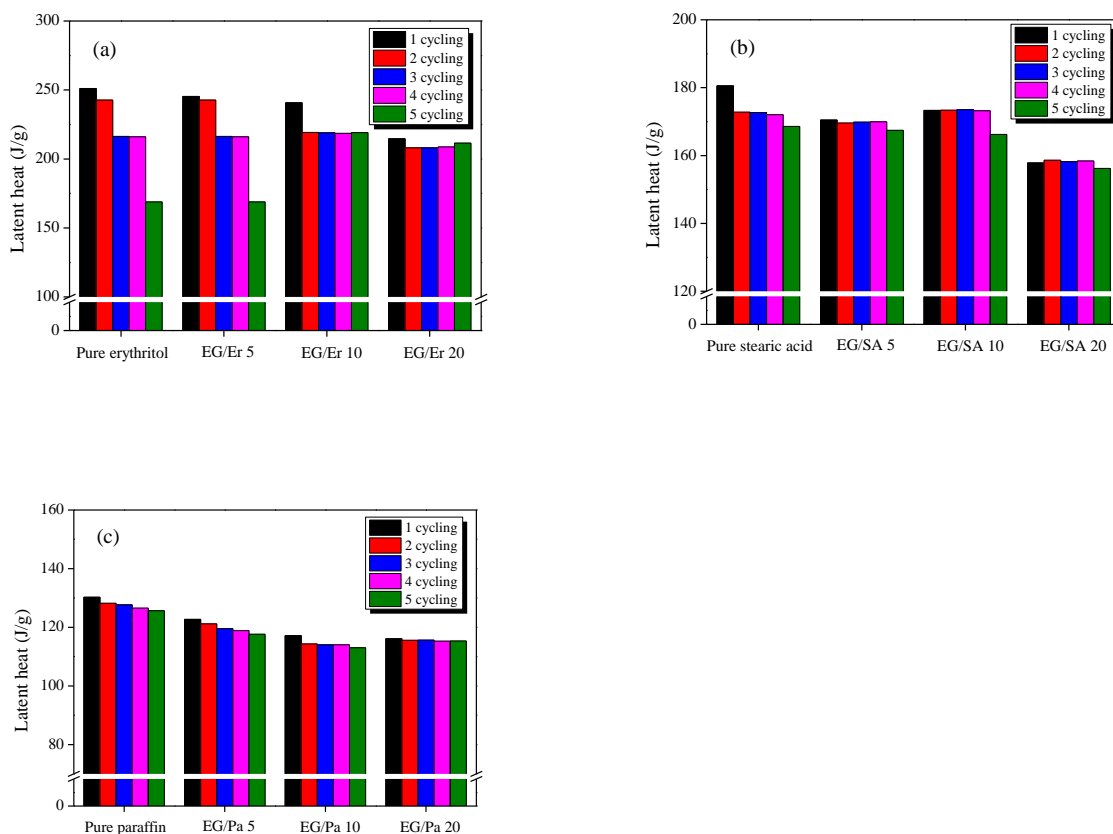
Fig.9 Thermal cycling tests of PCM composites as a function of EG content

Thermal stability of PCM composites

The weight loss of the PCM composites was shown in Fig. 10. As the EG loading increased, the thermal stability of EG/Er composites did not show significantly differ until 10 wt%, while at 20 wt% it slightly increased. Thermal decomposition of EG/Er composites gradually shifted to a higher temperature with increasing the EG content [40]. Although the interaction between graphite platelets and erythritol was weak, EG particles still interacted with surrounding matrix and improved the overall stability of the PCM composites.

The pure stearic acid started to be removed at about 170℃ and the final weight loss percentage was nearly 100% at 305℃. The TGA curves of EG/SA composites had similar weight loss behaviors. Most of the weight loss at temperatures of 170–305℃ was attributed to the removal of stearic acid in EG/SA composites which proceeded over a wider temperature range than that of pure stearic acid, probably because the EG layers could improve the thermal stability of stearic acid by creating a physical protective barrier on the surface of PCM composites. Similarly, in Fig. 10(c), thermal decomposition of EG/Pa composites gradually shifted to a higher temperature with increasing the EG content. It was significant that the weight loss of the PCM composites strongly depended on the loading ratios of PCM in the composites. Therefore, the PCM composites had a good thermal stability and could be used in thermal energy storage system.
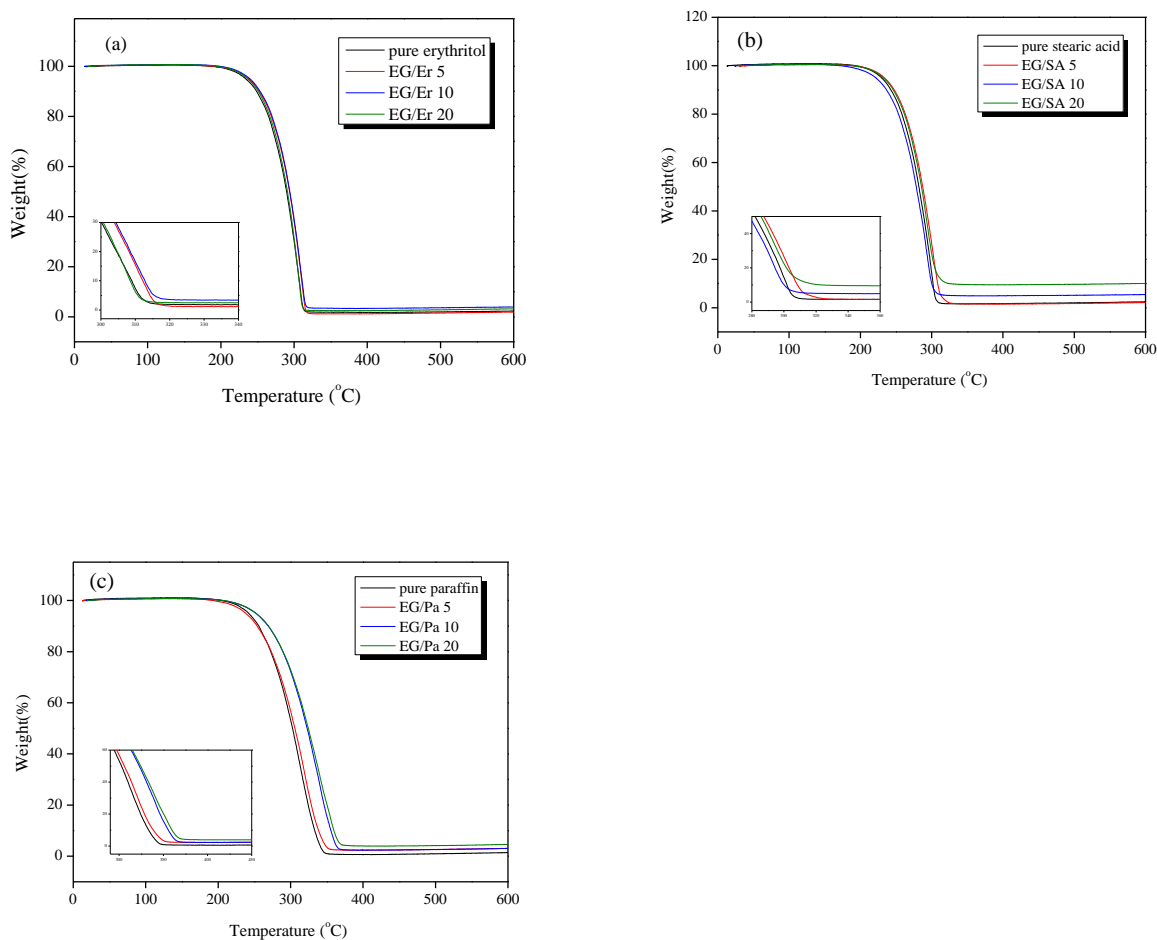
Fig.10 TGA curves of PCM composites as a function of EG content.

CONCLUSION

In this study, the thermal conductivity of the PCM composites was found to increase with loading of EG while the relative enhancement strongly depended on the high surface area and good dispersion. Among the three types of the PCM composites, EG/Er 20 showed the greatest increase of thermal conductivity and thermal diffusivity by 84.02% and 113.79%, which indicated their superior thermal cycling stability and response speed of the PCM composites. In contrast, the slightly decrease in energy storage capacity of the PCM composites from 251.08 to 214.58 J/g was owing to the presence of EG resulting from the decrement of super cooling effect.

In summary, the EG used as fillers was one of highly promising materials for preparing the PCM composites with greatly enhanced thermal conductivity and slightly decreased energy storage capacity which had great potential in thermal energy storage applications.

ACKNOWLEDGEMENTS

REFERENCES

[1] J. N. Shi, M. D. Ger, Y. M. Liu, Y. C. Fan, N. T. Wen, C. K. Lin, and N. W. Pu, Improving the thermal conductivity and shape-stabilization of phase change materials using nanographite additives, Carbon, vol. 51, pp. 365-372, 2013.

[2] P. M. Gilart, A. Y. Martinez, M. G. Barriuso, and C. M. Martinez, Development of PCM/carbon-based composite materials, Sol. Energy Mater. Sol. Cells, vol. 107, pp. 205-211, 2012.

[3] Y. Cai, Q. Wei, F. Huang, S. Lin, F. Chen, and W. Gao, Thermal stability, latent heat and flame retardant properties of the thermal energy storage phase change materials based on paraffin/high density polyethylene composites, Renew. Energy, vol. 34, pp. 2117-2123, 2009.

[4] Y. J. Chen, D. D. Nguyen, M. Y. Shen, M. C. Yip, and N. H. Tai, Thermal characterizations of the graphite nanosheets reinforced paraffin phase-change composites, Compos. A, vol. 44, pp. 40-46, 2013.

[5] S. Pincemin, R. Olives, X. Py, and M. Christ, Highly conductive composites made of phase change materials and graphite for thermal storage, Sol. Energy Mater. Sol. Cells, vol. 92, 603-613, 2008.

[6] T. Nomura, N. Okinaka, and T. Akiyama, Impregnation of porous material with phase change material for thermal energy storage, Master. Chem. Phys., vol. 115, pp. 846-850, 2009.

[7] A. A. Aydın and H. Okutan, High-chain fatty acid esters of myristyl alcohol with even carbon number: Novel organic phase change materials for thermal energy storage-1, Sol. Energy Mater. Sol. Cells, vol. 95, pp. 2752-2762, 2011.

[8] J. Zhu, L. Bai, B. Chen, and W. Fei, Thermodynamical properties of phase change materials based on ionic liquids, Chem. Eng. J., vol. 147, pp. 58-62, 2009.

[9] F. Frusteri, V. Leonardi, and G. Maggio, Numerical approach to describe the phase change of an inorganic PCM containing carbon fibres, Appl. Therm. Eng., vol. 26, pp. 1883-1892, 2006.

[10] A. Sarı, Thermal reliability test of some fatty acids as PCMs used for solar thermal latent heat storage applications, Energy Conv. Manag., vol. 44, pp. 2277-2287, 2003.

[11] M. Mehrali, S. T. Latibari, M. Mehrali, T. M. I. Mahlia, and H. S. C. Metselaar, Effect of carbon nanospheres on shape stabilization and thermal behavior of phase change materials for thermal energy storage, Energy Conv. Manag., vol. 88, pp. 206-213, 2014.

[12] J. Xiang, and L. T. Drzal, Investigation of exfoliated graphite nanoplatelets (xGnP) inimproving thermal conductivity of paraffin wax-based phase change material, Sol. Energy Mater. Sol. Cells, vol. 95, pp. 1811-1818, 2011.

[13] G. Fang, H. Li, Z. Chen, and X. Liu, Preparation and characterization of stearic acid/expanded graphite composites as thermal energy storage materials, Energy, vol. 35, pp. 4622-4626, 2010.

[14] G. Q. Qi, C. L. Liang, R. Y. Bao, Z. Y. Liu, W. Yang, B. H. Xie, and M. B. Yang, Polyethylene glycol based shape-stabilized phase change material for thermal energy storage with ultra-low content of graphene oxide, Sol. Energy Mater. Sol. Cells, vol. 123, pp. 171-177, 2014.

[15] M. E. Sotomayor, I. Krupa, A. Varez, and B. Levenfeld, Thermal and mechanical characterization of injection moulded high density polyethylene/paraffin wax blends as phase change materials, Renew. Energy, vol. 68, pp. 140-145, 2014.

[16] J. L. Zeng, J. Gan, F. R. Zhu, S. B. Yu, Z. L. Xiao, W. P. Yan, L. Zhu, Z. Q. Liu, L. X. Sun, and Z. Cao, Tetradecanol/expanded graphite composite form-stable phase change material for thermal energy storage, Sol. Energy Mater. Sol. Cells, vol. 127, pp. 122-128, 2014.

[17] S. Yu, S. G. Jeong, O. Chung, and S. Kim, Bio-based PCM/carbon nanomaterials composites with enhanced thermal conductivity, Sol. Energy Mater. Sol. Cells, vol. 120, pp. 549-554, 2014.

[18] T. Oya, T. Nomura, N. Okinaka, and T. Akiyama, Phase change composite based on porous nickel and erythritol, Appl. Therm. Eng., vol. 40, pp. 373-377, 2012.

[19] D. H. Choi, J. H. Lee, H. R. Hong, and Y. T. Kang, Thermal conductivity and heat transfer performance enhancement of phase change materials (PCM) containing carbon additives for heat storage application, Int. J. Refrig., vol. 42, pp. 112-120, 2014.

[20] T. Nomura, N. Okinaka, and T. Akiyama, Impregnation of porous material with phase change material for thermal energy storage, Mater. Chem. Phys., vol. 115, pp. 846-850, 2009.

[21] L. Xia, P. Zhang, and R. Z. Wang, Preparation and thermal characterization of expanded graphite/paraffin composite phase change material, Carbon, vol. 48, pp. 2538-2548, 2010.

[22] Y. Zhong, S. Li, X. Wei, Z. Liu, Q. Guo, J. Shi, and L. Liu, Heat transfer enhancement of paraffin wax using compressed expanded natural graphite for thermal energy storage, Carbon, vol. 48, pp. 300-304, 2010.

[23] A. Sari and A. Karaipekli, Preparation, thermal properties and thermal reliability of palmitic acid/expanded graphite composite as form-stable PCM for thermal energy storage, Sol. Energy Mater. Sol. Cells, vol. 93, pp. 571-576, 2009.

[24] A. Sari and A. Karaipekli, Thermal conductivity and latent heat thermal energy storage characteristics of paraffin/expanded graphite composite as phase change material, Appl. Therm. Eng., vol. 27, pp. 1271-1277, 2007.

[25] H. Yin, X. Gao, J. Ding, and Z. Zhang, Experimental research on heat transfer mechanism of heat sink with composite phase change materials, Energy Conv. Manag., vol. 49, pp. 1740-1746, 2008.

[26] S. Y. Lee, H. K. Shin, M. R. Park, K. Y. Rhee, and S. J. Park, Thermal characterization of erythritol/expanded graphite composites for high thermal storage capacity, Carbon, vol. 68, pp. 67-72, 2014.

[27] Z. Zhang and X. Fang, Study on paraffin/expanded graphite composite phase change thermal energy storage material, Energy Conv. Manag., vol. 47, pp. 303-310, 2006.

[28] S. J. Park, K. S. Kim, and J. R. Lee, Thermal and mechanical interfacial properties of expanded graphite/epoxy composites, J. Korean Ind. Eng. Chem., vol. 15, pp. 493-498, 2004.

[29] T. Nomura, K. Tabuchi, C. Zhu, N. Sheng, S. Wang, and T. Akiyama, High thermal conductive, Appl. Energy, vol. 154, pp. 678-685, 2015.

[30] L. Zhong, X. Zhang, Y. Luan, G. Wang, Y. Feng, and D. Feng, Preparation and thermal properties of porous heterogeneous composite phase change materials based on molten salts/expanded graphite, Sol. Energy, vol. 107, pp. 63-73, 2014.

[31] Z. Zhang, N. Zhang, J. Peng, X. Fang, X. Gao, and Y. Fang, Preparation and thermal energy storage properties of paraffin/expanded graphite composite phase change material, Appl. Energy, vol. 91, pp. 426-431, 2012.

[32] B. K. Choi, W. K. Choi, Y. S. Kuk, H. G. Kim, and M. K. Seo, A Study on Thermal Behaviors of Expanded Graphite/Erythritol Composites, Appl. Chem. Eng., vol. 25, pp. 463-467, 2014.

[33] J. Yang, E. Zhang, X. Li, Y. Zhang, J. Qu, and Z. Z. Yu, Cellulose/graphene aerogel supported phase change composites with high thermal conductivity and good shape stability for thermal energy storage, Carbon, vol. 98, pp. 50-57, 2016.

[34] S. Kim and L. T. Drzal, High latent heat storage and high thermal conductive phase change materials using exfoliated graphite nanoplatelets, Sol. Energy Mater. Sol. Cells, vol. 93, pp. 136-142, 2009.

[35] L. W. Fan, X. Fang, X. Wang, Y. Zeng, Y. Q. Xiao, Z. T. Yu, X. Xu, Y. C. Hu, and K. F. Cen, Effects of various carbon nanofillers on the thermal conductivity and energy storage properties of paraffin-based nanocomposite phase change materials, Appl. Energy, vol. 110, pp. 163-172, 2013.

[36] W. Wang, X. Yang, Y. Fang, J. Ding, and J. Yan, Preparation and thermal properties of polyethylene glycol/expanded graphite blends for energy storage, Appl. Energy, vol. 86, pp. 1479-1483, 2009.

[37] J. Jeon, S. G. Jeong, J. H. Lee, J. Seo, and S. Kim, High thermal performance composite PCMs loading xGnP for application to building using radiant floor heating system, Sol. Energy Mater. Sol. Cells, vol. 101, pp. 51-56, 2012.

[38] J. Jhao, Y. Guo, F. Feng, Q. Tong, W. Qv, and H. Wang, Microstructure and thermal properties of a paraffin/expanded graphite phase-change composite for thermal storage, Renew. Energy, vol. 36, pp. 1339-1342, 2011.

[39] Z. Wang, H. Wang, X. Li, D. Wang, Q. Zhang, G. Chen, and Z. Ren, Aluminum and silicon based phase change materials for high capacity thermal energy storage, Appl. Therm. Eng., vol. 89, pp. 204-208, 2015.

[40] Li, T. Liu, L. Hu, Y. Wang, and S. Nie, Facile preparation and adjustable thermal property of stearic acid–graphene oxide composite as shape-stabilized phase change material, Chem. Eng. J., vol. 215, pp. 819-826, 2013.